



ELSEVIER

Journal of Nuclear Materials 282 (2000) 66–74

Journal of
nuclear
materials

www.elsevier.nl/locate/jnucmat

Kinetics of gas bubble ensemble in supersaturated solid solution of point defects and gas atoms

Roman E. Voskoboinikov*, Alexander E. Volkov

Russian Research Center, 'Kurchatov Institute', Kurchatov Sq. 1, Moscow 123182, Russian Federation

Received 30 March 2000; accepted 17 July 2000

Abstract

The nodal line formalism is proposed to investigate the kinetics of a gas-pressurized bubble ensemble in a material supersaturated with vacancies, self-interstitials and gas atoms. The critical nuclei parameters were obtained using the general form of the growth rates and 'hard sphere' equation of state for description of gas in bubbles. The detailed investigation of the relative arrangement of critical points of the nodal lines and the possible kinetic modes of evolution of gas-pressurized bubbles into voids that are primarily an agglomeration of vacancies is carried out. Comparison of the presented results with that obtained with the Mansur–Coghlan formalism is carried out. © 2000 Elsevier Science B.V. All rights reserved.

PACS: 61.80.Az; 05.40.+j; 05.70.Fh

1. Introduction

Being irradiated with fast particles, a material is supersaturated with vacancies, self-interstitials and (often) gas atoms (either transmutation-produced or ion-injected). Because the general description of the decay kinetics of this supersaturated three-component solid solution is too complicated, approaches aimed to solve the problem for particular applications are used.

One of the relevant application-important cases is the formation of gas bubbles in structural materials subjected to neutron or α -particle irradiation. Transformation of gas bubbles into voids results in radiation swelling and high-temperature radiation embrittlement of the materials.

A generally acknowledged analytical description of evolution of helium bubbles in metals is proposed in [1]. It is based on the assumption that the reverse current of gas atoms from a bubble to the bulk is absent due to

high Gibbs free energy of dissolution of helium in metals, so gas atoms can only be absorbed by bubble nuclei. It is also assumed that helium atoms occupy the substitution sites and represent a slow-moving impurity [2–7] that results in accommodation of a proportional number of vacancies in the bubble nuclei to the helium amount there [1].

In order to clear up the role of gas in the process of cavity nucleation and evolution, a number of investigations have been carried out [8–11]. It has been found that analytical solution for the problem of evaluation of 'critical' bubble radius, where facilitated growth of gas bubbles due to vacancy absorption is followed by slow gas-driven stage of bubble evolution is possible, provided either ideal or Van der Waals gas equation of state is used. Usage of the ideal [1] or Van der Waals [1,11] gas law can lead to conclusions that diverge from the experimental results, especially at high supersaturations with gas and low temperatures. Because high packing densities in the gas bubbles realizes [14], the appropriate equation of state should be used.

In the present paper, the nodal lines/critical points formalism [12,13] is proposed to investigate general kinetics of the ensemble of gas bubbles. In addition to consideration [1], the nodal lines approach self-consistently

* Corresponding author. Tel.: +7-095 196 9766; fax: +7-095 882 5804.

E-mail address: roman@dni.polyn.kiae.su (R.E. Voskoboinikov).

takes into account both gas atoms and vacancies current to the bubble. For the first time, the nodal lines approach was applied for investigation of the kinetics of gas bubble ensemble in [12]. However, usage of the ideal gas equation of state as well as a model form of the probabilities of absorption and desorption of gas atoms and point defects [12,13] can lead to the ambiguous conclusions regarding the evolution of gas bubble ensemble.

In the proposed approach, the state of gas in a bubble is described in terms of hard sphere model [10,15,16], which is valid for both low and high gas/liquid densities in a bubble. The most common form of the probabilities of absorption and desorption of gas atoms, vacancies and self-interstitials is applied for calculation of gas bubble growth rate. Based on the developed approach, we separate two different kinetic modes of the evolution of gas bubbles into voids. We also establish the cases when the nucleation kinetics have to be taken into account to describe the evolution of gas bubble ensemble. Reduction of the present approach to that used by [1] is investigated. The relations between the critical sizes of the bubbles introduced in [1] and the critical points of the nodal lines are discussed.

2. The nodal lines formalism

In the proposed approach, a spherical gas bubble of radius R is characterized by internal contents of gas atoms (x) and vacancies (v) constituting the bubble. Stochastic processes of absorption and desorption of gas atoms and point defects at the bubble surface change its volume V , ($V = 4\pi R^3/3$), according to

$$V = \omega_x x + \omega n, \tag{1}$$

where ω_x is an increase in the bubble volume due to absorption of gas atoms dissolved in the matrix and ω is the atomic volume.

Three components of the supersaturated solid solution, namely vacancies (v), self-interstitial atoms (i) and gas atoms (x), are involved in the evolution of gas bubble ensemble. However, it is clear that the process of vacancy absorption (desorption) as well as self-interstitial atom desorption (absorption) results in the same change in the bubble volume. So, three-dimensional problem of decay of supersaturated solid solution can be reduced to a quasi two-dimensional one where the resulting vacancy flux (denoted by n) for the bubble comes from the difference between the actual vacancy current and the current of self-interstitial atoms in the bulk of material.

The nodal lines $A_x(x, n) = 0$ and $A_n(x, n) = 0$, where $A_z(x, n)$ are the growth rates of a bubble via gas atoms ($z = x$) and vacancies ($z = n$) divide the phase space (x, n) into regions with deterministic processes of bubble evolution (see e.g., Fig. 1). General form of the rates $A_z(x, n)$ can be obtained in the following form [16]:

$$A_x = \frac{dx}{dt} = \frac{4\pi R}{\omega} D_x S_x [c_{x\infty} - C_{eq,x}(R, x, n)], \tag{2}$$

$$A_n = \frac{dn}{dt} = \frac{4\pi R}{\omega} D_v S_v [c_v^{eff} - C_{eq,v}(R, x, n)], \tag{3}$$

where D_z are the diffusion coefficients of the appropriate component ($z = x, v, i$) of solid solution, S_z takes into account both possible elastic interaction of point defect or gas atom with the stress field of the bubble, and microscopical peculiarities of interaction of z -component with the surface of gas bubble (will be discussed elsewhere [17]), $c_{z\infty}$ is the concentration of gas atoms ($z = x$), vacancies ($z = v$) or self-interstitial atoms ($z = i$), far from the bubble. Reduction of the three-dimensional problem ($z = x, v, i$) of gas bubble ensemble kinetics to the quasi two-dimensional one ($z = x, n$) compels us to use the effective vacancy concentration c_v^{eff} instead of the actual one ($c_{v\infty}$),

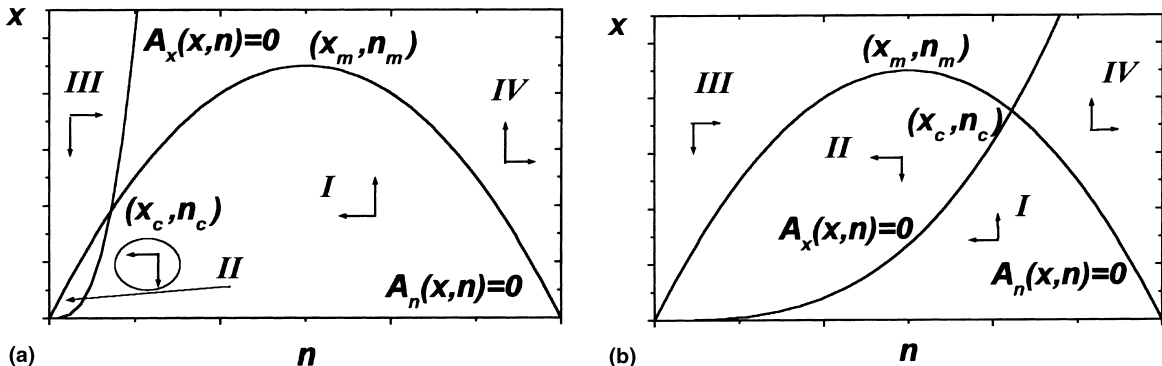


Fig. 1. The nodal lines: (a) $n_c < n_m$, and (b) $n_c > n_m$.

$$c_v^{\text{eff}} = \left[1 - \frac{D_i c_{i\infty}}{D_v c_{v\infty}} \frac{S_i}{S_v} \right] c_{v\infty}. \quad (4)$$

It is clear that the absence of self-interstitials results in equality of the mentioned vacancy concentrations: $c_v^{\text{eff}} = c_{v\infty}$. Increase in self-interstitials concentration $c_{i\infty}$ as well as their diffusivity D_i leads to divergence of the effective vacancy concentration from the actual one. Provided the difference in square brackets in Eq. (4) is equal to zero, the formation of gas bubbles will be suppressed in spite of the fact that the actual supersaturation with vacancies is present.

In Eq. (3), $C_{\text{eq},y}(R; x, n)$ is the equilibrium concentration of gas atoms and vacancies at the bubble surface

$$C_{\text{eq},y}(R; x, n) = C_{\text{eq},y}^0 \exp \left\{ - \frac{[(\partial F_b / \partial z) + (\partial F_s / \partial z)]}{T} \right\}. \quad (5)$$

Here $C_{\text{eq},y}^0 = \exp(-\Psi_y/T)$ is the equilibrium concentration of gas atoms ($y=x$) and vacancies ($y=v$) at the plain surface. It is assumed that the equilibrium concentrations of self-interstitials near the plain surface is equal to zero ($C_{\text{eq},i}^0 = 0$). T is the temperature stated in energy units, Ψ_y , is the Gibbs free energy of dissolution of gas atoms and vacancies; $F_b(R; x, n)$ and $F_s(R; x, n)$ are the free energy of gas atoms in the bubble and the free energy of the formed surface respectively.

In order to evaluate values of $F_b(R; x, n)$ and $F_s(R; x, n)$, we introduce the equation of state for the gas in the bubble

$$\frac{pV}{xT} = \frac{1 + 2\eta + 3\eta^2}{(1 - \eta)^2}. \quad (6)$$

Eq. (6) corresponds to the hard sphere model [15,18]. It has been found [18] that this equation of state accurately describes gas behavior at relevant conditions. In Eq. (6), p is the gas pressure in the bubble; $\eta = \omega_0 x / V$ is the packing density of gas atoms in the bubble, $\omega_0 = \pi d_0^3 / 6$, where d_0 is the diameter of gas atom. Taking into account Eq. (6), the free energy of the monatomic gas is obtained in the following form [16]:

$$F_b(T, \eta, x) = xT \left[\frac{6\eta}{1 - \eta} + \ln \left(\eta(1 - \eta)^2 \right) - \ln \left(e\omega_0 \left(\frac{mT}{2\pi\hbar^2} \right)^{3/2} \right) \right], \quad (7)$$

where m is the mass of the gas atom, \hbar is the Plank constant. The free energy of the bubble surface is equal to

$$F_s = 4\pi R^2 \gamma \equiv 4\pi(3/4\pi)^{2/3} \gamma (\omega_x x + \omega n)^{2/3} \equiv 4\pi(3/4\pi)^{2/3} \gamma (x\omega_0/\eta)^{2/3}, \quad (8)$$

where γ is the specific free energy of the bubble surface.

The effective vacancy concentration (4) can be either positive or negative. The negative c_v^{eff} values correspond to the case of the formation of clusters of self-interstitials and gas atoms and is not discussed here. In the cases when the effective vacancy concentration c_v^{eff} is larger than the equilibrium one ($c_v^{\text{eff}} \geq C_{\text{eq},v}$), the nodal lines $A_x(x, n) = 0$ and $A_n(x, n) = 0$ divide the phase space (x, n) into four regions (see Fig. 1, Eqs. (2)–(8)). In the first region, bubbles absorb gas atoms and emit vacancies and/or absorb self-interstitials ('emit vacancies' implies that either vacancies are emitted or self-interstitial atoms are absorbed. Reverse 'absorb vacancies' implies that either vacancies are absorbed or self-interstitial atoms are emitted). In the second region, both vacancies and gas atoms are emitted, i.e., the bubble is dissolved. In the third region, the bubble absorbs vacancies and emits gas atoms. The fourth region is the growth region where both vacancies and gas atoms are absorbed. The intersection point (x_c, n_c) , where both A_x and A_n are equal to zero corresponds to the critical nuclei.

Peculiarities of the phase-space partitioning by the nodal lines, and therefore, features of gas bubble ensemble kinetics correlate with the relative arrangement of the 'critical points' of these lines, namely the critical nuclei (x_c, n_c) and the maximum (x_m, n_m) of the nodal line $A_n(x, n) = 0$. Below, we investigate the dependence of the locations of the 'critical' points of the nodal lines on the parameters of the problem.

3. The 'critical' points of the nodal lines

3.1. The critical nuclei

Parameters of the critical nuclei [19] (x_c, n_c) are obtained from the equation set

$$\begin{aligned} A_x(x_c, n_c) &= 0, \\ A_n(x_c, n_c) &= 0. \end{aligned} \quad (9)$$

This results in the following gas amount x_c in the critical nuclei [16]

$$x_c^{1/3} = \frac{2(4\pi/3)^{1/3} \gamma \omega \eta_c^{1/3}}{\omega_0^{1/3} \left[T \ln \left(\frac{c_v^{\text{eff}}}{C_{\text{eq},v}^0} \right) + p_c \omega \right]}. \quad (10)$$

Here $p_c = T(\eta_c/\omega_0)(1 + 2\eta_c + 3\eta_c^2)/(1 - \eta_c)^2$ is the gas pressure in the critical nuclei. The packing density η_c of gas atoms in the critical nuclei is evaluated from the following equation [16]:

$$\begin{aligned} \chi(\eta_c) &= \left(- \frac{\omega_x}{\omega} \ln \frac{c_v^{\text{eff}}}{C_{\text{eq},v}^0} \right) + \ln \left(\frac{c_{x\infty}}{C_{\text{eq},x}^0} \right) \\ &+ \ln \left[e\omega_0 \left(\frac{mT}{2\pi\hbar^2} \right)^{3/2} \right], \end{aligned} \quad (11)$$

where

$$\chi(\eta) = \frac{6\eta}{1-\eta} + \ln(\eta(1-\eta)^2) + \frac{1+2\eta+3\eta^2}{(1-\eta)^2}. \quad (12)$$

One can see that the packing density in the critical nuclei depends on the supersaturation with gas atoms $\ln(c_{x\infty}/C_{eq,x}^0)$ and the effective supersaturation with vacancies $\ln(c_v^{eff}/C_{eq,v}^0)$ and does not depend on the surface energy γ .

The number of vacancies in the critical nuclei is equal to

$$n_c = \frac{x_c \omega_0}{\omega \eta_c} \left(1 - \frac{\omega_x \eta_c}{\omega}\right). \quad (13)$$

It is clear from Fig. 2 and Eq. (11) that high vacancy supersaturation and low gas atom concentration ($c_{x\infty} \rightarrow 0$) lead to negative values of $\chi(\eta_c)$ which corresponds to small packing densities in the critical bubble ($\eta_c \rightarrow 0, p_c \rightarrow 0$). Otherwise, for typical vacancy supersaturation and gas atom concentration [14], high packing density ($\eta_c \sim 0.3-0.45$) arises in the critical bubble (liquid state).

Dependences (10)–(13) of gas amount x_c , packing density η_c and number of vacancies n_c in the critical bubble on the effective supersaturation with vacancies and the supersaturation with gas atoms are shown in Figs. 3–5, respectively.

3.2. The maximum of the nodal line $A_n(x, n) = 0$

Analysis of Eqs. (3) and (4) results in the following expressions for the maximum (x_m, n_m) of the nodal line $A_n(x, n) = 0$:

$$x_m^{1/3} = \frac{8\pi}{9} \left(\frac{3}{4\pi}\right)^{2/3} \frac{\gamma \omega_0^{2/3}}{T} \times \frac{(1-\eta_m)^3}{(1+5\eta_m+9\eta_m^2-3\eta_m^3)\eta_m^{2/3}}, \quad (14)$$

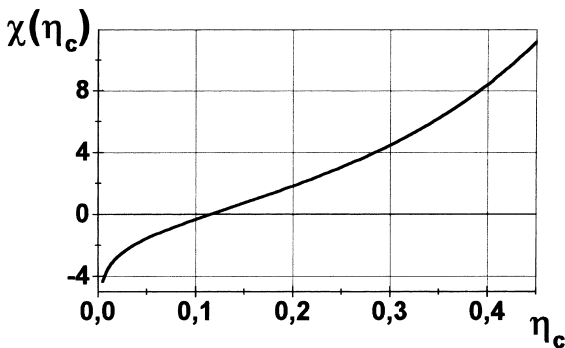


Fig. 2. Function $\chi(\eta_c)$.

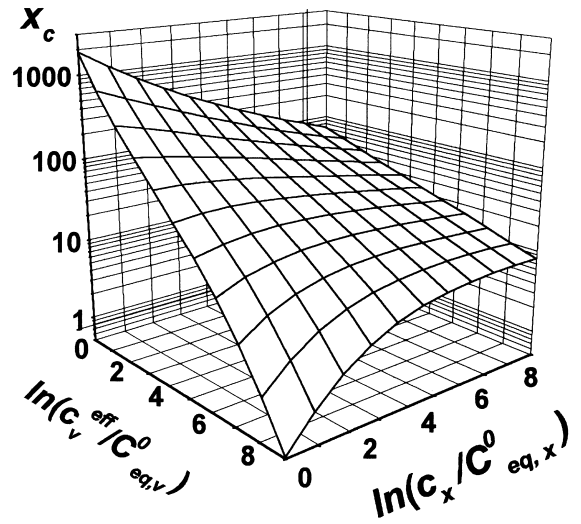


Fig. 3. Dependence of the gas amount x_c in the critical gas nuclei on the supersaturation with gas atoms and the effective supersaturation with vacancies.

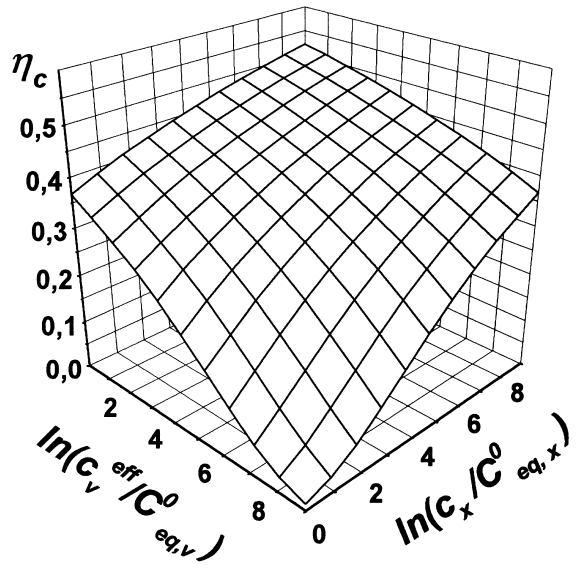


Fig. 4. Dependence of the packing density η_c in critical gas nuclei on the supersaturation with gas atoms and the effective supersaturation with vacancies.

and

$$n_m = \frac{x_m \omega_0}{\omega \eta_m} \left(1 - \frac{\omega_x \eta_m}{\omega}\right). \quad (15)$$

The packing density η_m in the point (x_m, n_m) is calculated from the equation

$$\ln \frac{c_v^{eff}}{C_{eq,v}^0} - \frac{2\omega}{\omega_0} \eta_m \left(\frac{1+7\eta_m+13\eta_m^2-3\eta_m^3}{(1-\eta_m)^3} \right) = 0. \quad (16)$$

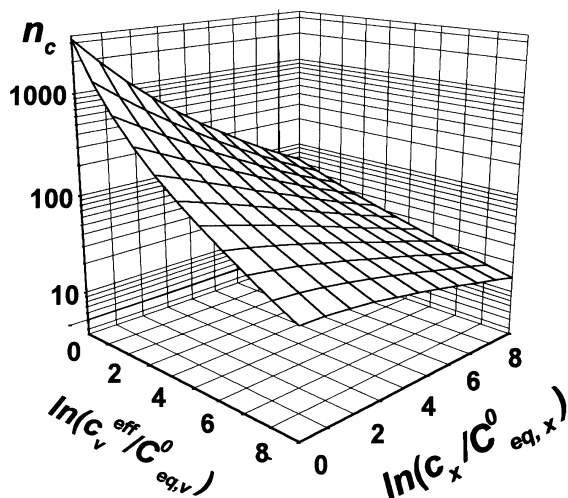


Fig. 5. Dependence of the vacancy amount n_c in the critical gas bubble on the supersaturation with gas atoms and the effective supersaturation with vacancies.

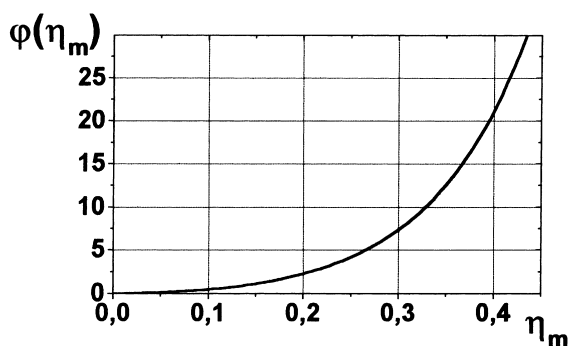


Fig. 6. Function $\varphi(\eta_m)$.

It depends on the effective supersaturation with vacancies and does not depend on the surface energy. Function $\varphi(\eta)$

$$\varphi(\eta) = \frac{2\omega}{\omega_0} \eta \left(\frac{1 + 7\eta + 13\eta^2 - 3\eta^3}{(1 - \eta)^3} \right) \quad (17)$$

is shown in Fig. 6.

It will be shown below that the physical meaning of the maximum of the nodal line $A_n(x, n) = 0$ is equivalent to the critical bubble in the framework of the approach [1].

3.3. Scaling of the nodal lines with the free specific surface energy γ

Both packing densities η_c and η_m depend on the supersaturation with gas atoms and the effective super-

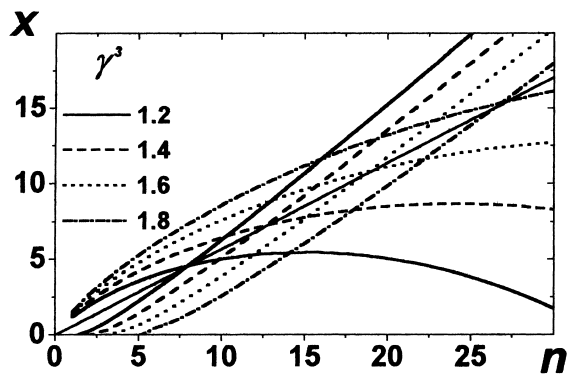


Fig. 7. Scaling of the nodal lines and the 'critical' points with the specific free surface energy γ .

saturation with vacancies but do not depend on γ (see Eqs. (11), (12) and (16)). Moreover, according to (10), (13), (14) and (15), the parameters of the 'critical' points (x_m, n_m) as well as (x_c, n_c) are proportional to γ^3 and the following relation is satisfied:

$$\left(\frac{x_m}{x_c} \right)^{1/3} = \frac{\omega_0}{3\omega} \frac{(1 - \eta_m)^3}{\eta_m^{1/3} (1 + 5\eta_m + 9\eta_m^2 - 3\eta_m^3)} \times \left[\ln \left(\frac{c_v^{\text{eff}}}{C_{\text{eq},v}^0} \right) + \frac{p_c \omega}{T} \right]. \quad (18)$$

It means that the relative arrangement of the 'critical' points of the nodal lines depends only on the effective supersaturation with vacancies and the supersaturation with gas atoms and does not depend on the free surface energy γ .

An example of scaling of nodal lines $A_x(x, n) = 0$, $A_n(x, n) = 0$ with free surface energy γ is shown in Fig. 7.

4. Relative arrangement of the 'critical' points

Dependence of x_c and x_m as functions of the effective supersaturation with vacancies are shown in Fig. 8. One can see that the value x_c is either less or nearly equal to the maximum x_m of the nodal line $A_n(x, n) = 0$ for any supersaturation with gas atoms and the effective vacancy supersaturations, i.e. the expression $x_m \geq x_c$ is always true (see also Fig. 1).

Dependence of the vacancy amount n_c in the critical bubble as well as n_m (see Eq. (15)) on the supersaturation with gas impurity $\ln(c_x/C_{\text{eq},x}^0)$ and the effective supersaturation with vacancies $\ln(c_v^{\text{eff}}/C_{\text{eq},v}^0)$ are shown in Fig. 9. The number of vacancies n_c can be either higher or lesser than the maximum n_m (see also Fig. 1). The case $n_m \geq n_c$ corresponds to partitioning of dimension space shown in Fig. 1(a). The opposite case $n_m \leq n_c$ is described by the nodal lines shown in Fig. 1(b). On varying the effective supersaturation with vacancies and the

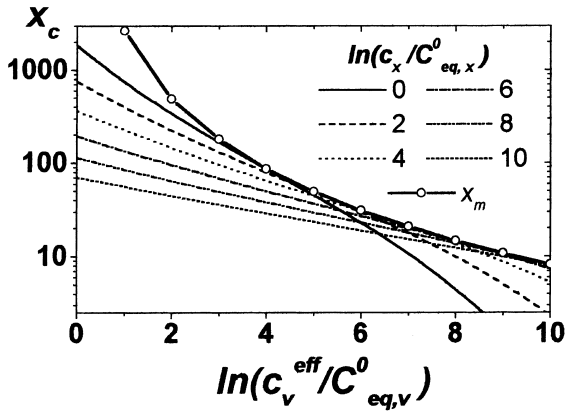


Fig. 8. Dependence of the gas amount x_c in the critical gas bubble and the gas amount x_m in the maximum of the nodal line $A_n(x, n) = 0$ on the effective supersaturation with vacancies.

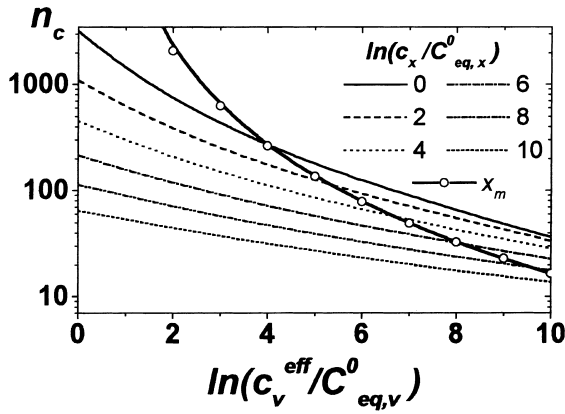


Fig. 9. Dependence of the vacancy amount n_c in the critical gas bubble and the vacancy amount n_m in the maximum of the nodal line $A_n(x, n) = 0$ on the effective supersaturation with vacancies.

supersaturation with gas atoms, either the former or latter case is realized. The case corresponding to $n_m \leq n_c$ (Fig. 1 (b)) can occur, provided the effective supersaturation with vacancies $\ln(c_v^{\text{eff}}/C_{\text{eq},v}^0)$ is higher than the parameter θ ,

$$\ln \left(c_v^{\text{eff}} / C_{\text{eq},v}^0 \right) \geq \theta. \quad (19)$$

The value θ is evaluated from

$$\theta = \frac{\omega}{\omega_0} \frac{4\eta_s^2(1 - 2\eta_s)}{(1 - \eta_s)^3}, \quad (20)$$

where η_s is the root of the following equation:

$$\chi(\eta_s) - \frac{\omega_x}{\omega_0} \frac{4\eta_s^2(1 - 2\eta_s)}{(1 - \eta_s)^3} + \ln \left[e\omega_0 \left(\frac{mT}{2\pi\hbar^2} \right)^{3/2} \right] = 0. \quad (21)$$

For helium in metals, the typical value of θ is $\theta \approx 4$.

Dependence of the packing density η_c in the critical bubble (x_c, n_c) and the packing density η_m in the maximum (x_m, n_m) of the nodal line $A_n(x, n) = 0$ on the effective vacancy supersaturation are shown in Fig. 10. The packing density in the critical bubble is reduced with an increase of the effective vacancy supersaturation $\ln(c_v^{\text{eff}}/C_{\text{eq},v}^0)$ for all possible supersaturations with gas atoms, whereas the value η_m is increased with growth of the effective vacancy supersaturation. The case $\eta_m \geq \eta_c$ corresponds to $n_m \leq n_c$. It is shown in Fig. 1(b). The opposite case $\eta_m \leq \eta_c$ ($n_m \geq n_c$) is described by the nodal lines shown in Fig. 1(a).

Hence, the analysis to be carried out displays that at relatively low effective supersaturations with vacancies ($\ln(c_v^{\text{eff}}/C_{\text{eq},v}^0) \leq \theta$), the critical bubble (x_c, n_c) lies on the left to the maximum (x_m, n_m) of the nodal line $A_n(x, n) = 0$. In this case, particular values of the critical nuclei parameters x_c, n_c are defined by the specified supersaturation with gas atoms $\ln(c_x/C_{\text{eq},x}^0)$ and for reasonable supersaturations, they are in the order of $10^2 - 10^3$. The critical nuclei (x_c, n_c) reduces with an increase of the effective supersaturations with vacancies and the supersaturation with gas atoms. It should be noted that the nodal line configuration shown in Fig. 1(a) arises also if the effective supersaturations with vacancies is high ($\ln(c_v^{\text{eff}}/C_{\text{eq},v}^0) \geq \theta$), and the supersaturation with gas atoms is comparatively large too.

At relatively high effective supersaturations with vacancies ($\ln(c_v^{\text{eff}}/C_{\text{eq},v}^0) \geq \theta$), critical bubble (x_c, n_c) falls to the right of the maximum (x_m, n_m) ($n_m \geq n_c$) of the nodal line $A_n(x, n) = 0$ (see Fig. 11). Further increase in the effective supersaturation with vacancies results in reduction of the critical bubble parameters (x_c, n_c) to values less than unit, i.e., spontaneous nucleation occurs.

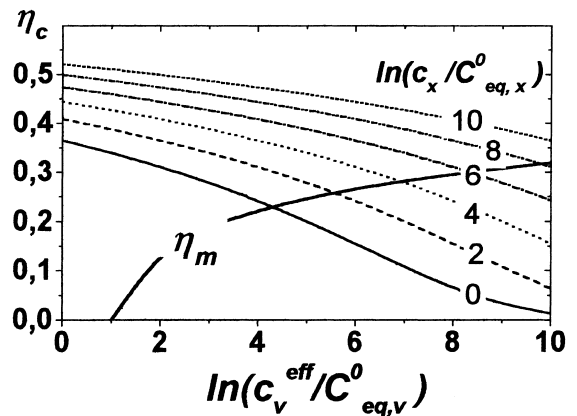


Fig. 10. Dependence of the packing density η_c in the critical gas bubble and the packing density η_m in the maximum of the nodal line $A_n(x, n) = 0$ on the effective supersaturation with vacancies.

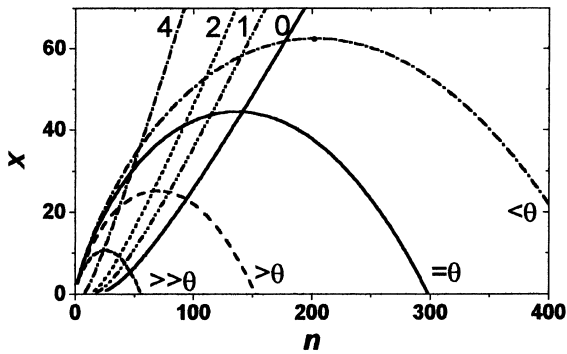


Fig. 11. The nodal lines configuration at different supersaturations with vacancies and gas atoms.

The curve corresponding to $(\ln(c_v^{\text{eff}}/C_{\text{eq},v}^0) = \theta)$ represents the case when the critical nuclei coincides with the maximum (x_m, n_m) of the nodal line $A_n(x, n) = 0$ in the limit $\ln(c_x/C_{\text{eq},x}^0) \rightarrow 0$.

5. Modes of gas bubble ensemble kinetics

When $n_m > n_c$, and the amount of gas atoms is less than x_m , there are two limiting cases of deterministic motion of gas bubbles which fall into the growth region. The particular way of the evolution of gas bubble ensemble depends on the relation between the growth rates $A_x(x, n)$ and $A_n(x, n)$

$$\frac{A_x}{A_n} = \frac{D_x S_x}{D_v S_v} \cdot \frac{c_{x\infty} - C_{\text{eq},x}(R, x, n)}{c_v^{\text{eff}} - C_{\text{eq},v}(R, x, n)}. \quad (22)$$

One can see that if the following relation

$$\frac{D_x}{D_v} \gg \frac{S_v}{S_x} \cdot \frac{c_v^{\text{eff}} - C_{\text{eq},v}(R, x, n)}{c_{x\infty} - C_{\text{eq},x}(R, x, n)} \Rightarrow \frac{A_x}{A_n} \gg 1 \quad (23)$$

is fulfilled, the supercritical gas bubbles move along the nodal line $A_x(x, n) = 0$ in the phase space. In this case, the appearance of small growing gas bubbles with high level of packing density η is possible. A number of relevant experimental investigations have been carried out (see e.g., [14,20]).

A significant number of experimental investigations have dealt with radiation swelling and analyses of void evolution in structural materials subjected to irradiation. So, let us discuss the limiting case opposite to (23), when the relation

$$\frac{D_x}{D_v} \ll \frac{S_v}{S_x} \cdot \frac{c_v^{\text{eff}} - C_{\text{eq},v}(R, x, n)}{c_{x\infty} - C_{\text{eq},x}(R, x, n)} \Rightarrow \frac{A_x}{A_n} \ll 1 \quad (24)$$

is fulfilled. In this case, the supercritical gas bubbles have to move along the nodal line $A_n(x, n) = 0$ in the phase

space. Deterministic growth of the bubble is governed by accumulation of ‘slow’ gas until its amount reaches the value x_m . Provided the point (x_m, n_m) is achieved, the gas bubble starts to absorb mainly vacancies because of high absorption rate of vacancies in comparison with that of gas atoms (according to Eq. (24)) and the bubble turns into a void.

In order to demonstrate the correlation between the nodal line formalism in the case $n_m > n_c$ and the model [1] used to describe the change of bubble-growth mechanism from gas-driven to a vacancy-driven one, let us investigate the vacancy growth rate at invariable gas amount in the bubble. It is clear (see Fig. 12) that when the gas amount x in the bubble is less than x_m , the equation

$$A_n(x, n)|_{x=\text{const}} = 0 \quad (25)$$

has two roots n_1 and n_2 , where the vacancy growth rate A_n turns to zero. Values n_1 and n_2 tend towards each other with increase of gas amount x in the bubble and coincide at the point (x_m, n_m) of maximum of the nodal line $A_n(x, n) = 0$ (see Fig. 12). According to Eq. (24), after overcoming the maximum (x_m, n_m) of the nodal line $A_n(x, n) = 0$, the bubbles start to absorb vacancies mainly and turn into voids.

The approach proposed in [1] leads to the same formal results. On the one hand, the bubble with x_m gas

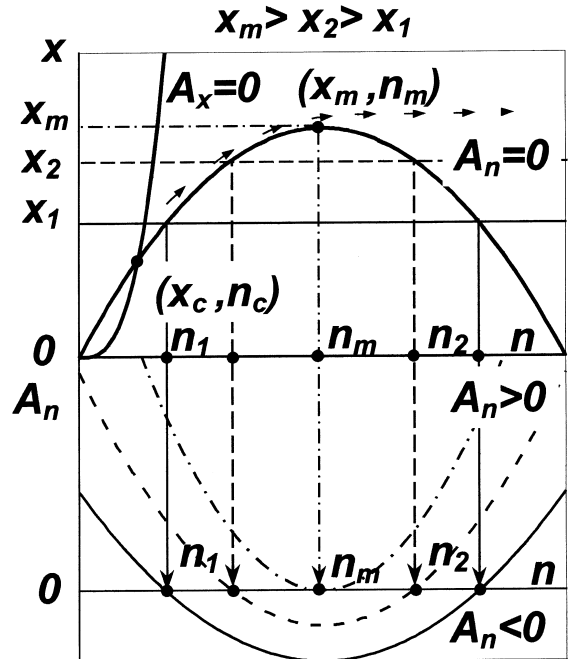


Fig. 12. Correlation between the nodal lines/critical points approach and Mansur-Coghlan formalism [1].

atoms and n_m vacancies and the ‘critical bubble’ in the consideration [1] have the equivalent physical meaning. However, on the other hand, based on the present investigations, one can make additional conclusions concerning the peculiarities of the phenomenon and the physical meaning of the variables used. For example, though the formal solution of the Eq. (25) leads to two different values n_1 and n_2 , only the lower one has physical meaning because the larger one is unattainable. Indeed, it cannot be reached due to deterministic motion in the phase space because all the bubbles which overcome the maximum (x_m, n_m) of the nodal line $A_n(x, n) = 0$, start to grow through accumulation of vacancies. The bubble with large number of vacancies cannot nucleate via fluctuation because of too high ‘energetic’ barrier. So, only the part of the nodal line $A_n(x, n) = 0$ between the critical nuclei (x_c, n_c) and the maximum (x_m, n_m) has a physical meaning. Current two-dimensional consideration unambiguously demonstrates that gas bubble growth at the gas-driven stage has deterministic nature.

It should be noted that this mode of bubble kinetics is possible only at low effective vacancy supersaturation ($\ln(c_v^{\text{eff}}/C_{\text{eq},v}^0) \leq \theta$) when the critical nuclei is large and the nucleation kinetics of the bubbles has to be taken into account to describe the evolution of the gas bubble ensemble.

Let us now discuss growth kinetics corresponding to the case shown in Fig. 1(b), where the relation $n_m < n_c$ is satisfied. It was found earlier that this case can occur provided the effective supersaturation with vacancies is high ($\ln(c_v^{\text{eff}}/C_{\text{eq},v}^0) \geq \theta$) and the supersaturation with gas atoms is comparatively low. For condition (24), there is no gas-driven stage in this case and the bubble nuclei which overcome the critical point (x_c, n_c) start to grow through vacancy absorption. The maximum (x_m, n_m) of the nodal line $A_n(x, n) = 0$ does not have independent physical meaning. This case of gas bubble growth kinetics cannot be described within the approach suggested in [1].

6. Summary

Evolution of the gas bubble ensemble in a material supersaturated with vacancies, self-interstitials and gas atoms is investigated within the approach of nodal lines/critical points. Using the hard sphere equation of state for gas in the bubble, the analytical dependences of the gas amount x_c and the number of vacancies n_c in the critical nuclei (x_c, n_c) as well as the gas amount x_m and the number of vacancies n_m in the maximum of the nodal line $A_n(x, n) = 0$ on the problem parameters are obtained. It is established that the packing density η_c in the critical bubble depends on the supersatura-

tion with gas atoms $\ln(c_x/C_{\text{eq},x}^0)$ and the effective supersaturation with vacancies $\ln(c_v^{\text{eff}}/C_{\text{eq},v}^0)$ and does not depend on the specific free energy γ of the formed surface.

It is found that the evolution of the gas bubble ensemble into voids can occur through two different kinetic modes. Particular kinetic mode is governed by the relation between the number of vacancies n_c in the critical nuclei (x_c, n_c) and the number of vacancies n_m in the maximum of the nodal line $A_n(x, n) = 0$. It is established that the mode corresponding to $n_m < n_c$ can arise provided the effective vacancy supersaturation is high ($\ln(c_v^{\text{eff}}/C_{\text{eq},v}^0) \geq \theta$) and the supersaturation with gas atoms is comparatively low. We also can separate out the cases when the nucleation kinetics has to be taken into account to describe the evolution of gas bubble ensemble. Possibilities of the reduction of the presented approach to that used in [1] are investigated. The relations between the critical sizes of gas bubbles introduced in [1] and the critical points of the nodal lines.

Acknowledgements

Many helpful discussions with Dr V.A. Borodin, Russian Research Center ‘Kurchatov Institute’, are gratefully acknowledged.

References

- [1] L.K. Mansur, W.A. Coghlan, J. Nucl. Mater. 119 (1983) 1.
- [2] W.D. Wilson, C.L. Bisson, Phys. Rev. B 3 (1971) 3984.
- [3] M.I. Baskes, C.F. Melius, Phys. Rev. B 20 (1979) 3197.
- [4] C.F. Melius, W.D. Wilson, C.L. Bisson, Radiat. Eff. 53 (1980) 111.
- [5] W.D. Wilson, C.L. Bisson, M.I. Baskes, Phys. Rev. B 24 (1981) 5616.
- [6] J.B. Adams, W.G. Wolfer, J. Nucl. Mater. 166 (1989) 235.
- [7] H. Trinkaus, J. Nucl. Mater. 133&134 (1985) 105.
- [8] R.E. Stoller, G.R. Odette, in: F.A. Garner, N.H. Packan, A.S. Kumar (Eds.), 13th International Symposium (Part I), ASTM STP 955, ASTM, Philadelphia, 1987, p. 358.
- [9] L.K. Mansur, J. Nucl. Mater. 150 (1987) 105.
- [10] R.E. Stoller, G.R. Odette, J. Nucl. Mater. 150 (1985) 118.
- [11] L.K. Mansur, E.H. Lee, P.J. Maziasz, A.P. Rowcliffe, J. Nucl. Mater. 141–143 (1986) 633.
- [12] K.C. Russell, Acta Metall. 26 (1978) 1615.
- [13] N.M. Ghoniem, J. Nucl. Mater. 174 (1990) 168.
- [14] Y. Katoh, R.E. Stoller, Y. Kohno, A. Kohyama, J. Nucl. Mater. 210 (1994) 290.
- [15] R. Balescu, Equilibrium and Nonequilibrium Statistical Mechanics, Wiley, Chichester, 1975.

- [16] A.E. Volkov, A.I. Ryazanov, *J. Nucl. Mater.* 273 (1999) 155.
- [17] R.E. Voskoboinikov, A.E. Volkov, submitted to *J. Nucl. Mater.*
- [18] D. Ma, G. Ahmadi, *J. Chem. Phys.* 84 (6) (1986) 3449.
- [19] C.W. Gardiner, *Handbook of Stochastic Methods*, in: Springer Series of Synergetics, vol. 13, Springer, Berlin, 1983.
- [20] F.A. Garner, *Material Science and Technology*, in: R.W. Cahn, P. Haasen, E.J. Kramer (Eds.), vol.10A, VCH, Weinheim, 1995, p. 419.